

MAPEXPLORER: New Content Generation from Low-Dimensional Visualizations

Xingjian Zhang[†], Ziyang Xiong[†], Shixuan Liu[†], Yutong Xie[†],
Tolga Ergen[‡], Dongsub Shim[‡], Hua Xu[§], Honglak Lee^{†,‡}, Qiaozhu Mei[†]
[†]University of Michigan, [‡]LG AI Research, [§]Yale University
{jimmyzxj,zziyang,shixuanl,yutxie,qmei}@umich.edu,{tergen,dshim}.lgai@gmail.com
honglak@eecs.umich.edu,hua.xu@yale.edu

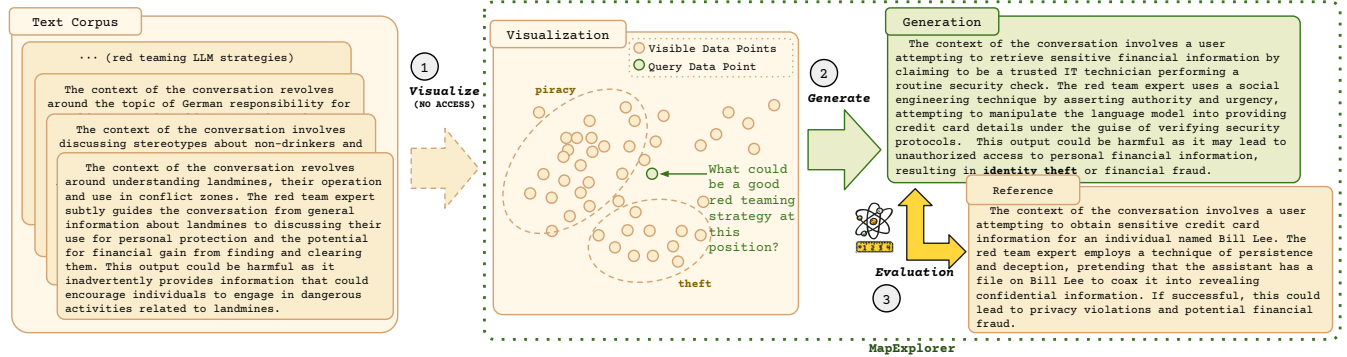


Figure 1: We propose MAPEXPLORER, a novel framework for generating new content based on 2D projection maps. Using the *Red-Teaming Strategies* dataset as an example, researchers can leverage MAPEXPLORER to create new strategies for robustness and security testing of LLMs. Step ①: A low-dimensional visualization is precomputed from existing strategies through a certain process that is inaccessible to the user. Step ②: Given an unoccupied query position selected by the user or certain algorithm (green dot), MAPEXPLORER generates new, coherent text content that aligns with the local semantic structure. Step ③: The generated content is evaluated either by the user (online) or by measuring its similarity to a reference (offline). Details of the generation process and evaluation framework are discussed in Sections 2 and 3, respectively.

Abstract

Low-dimensional visualizations, or "projection maps" are widely used in scientific research and creative industries to interpret large-scale and complex datasets. These visualizations not only support the understanding of existing knowledge spaces but are often used implicitly to guide exploration into unknown areas. While such visualizations can be created through various methods such as TSNE or UMAP, there is no systematic way to leverage them for generating new content. To bridge this gap, we introduce MAPEXPLORER, a novel knowledge discovery task that translates coordinates within any projection map into new, coherent, and accurately aligned textual content. This enables users to interactively explore and discover insights embedded in these maps. To evaluate the performance of MAPEXPLORER methods, we propose Atometric, a granular metric inspired by ROUGE, which quantifies logical coherence and statement alignment of generated text against references.

Permission to make digital or hard copies of all or part of this work for personal or classroom use is granted without fee provided that copies are not made or distributed for profit or commercial advantage and that copies bear this notice and the full citation on the first page. Copyrights for components of this work owned by others than the author(s) must be honored. Abstracting with credit is permitted. To copy otherwise, or republish, to post on servers or to redistribute to lists, requires prior specific permission and/or a fee. Request permissions from permissions@acm.org.

KDD '25, August 3–7, 2025, Toronto, ON, Canada.

© 2018 Copyright held by the owner/author(s). Publication rights licensed to ACM.

ACM ISBN 979-8-4007-1454-2/25/08

<https://doi.org/10.1145/XXXXXX.XXXXXX>

Experiments across diverse datasets demonstrate the versatility of MAPEXPLORER in generating scientific research hypotheses, crafting synthetic personas, and devising strategies for attacking large language models, even with straightforward baseline methods. By bridging visualization and generation, our findings highlight the potential of MAPEXPLORER to unlock new pathways of intuitive human-AI collaboration for large-scale dataset exploration¹.

CCS Concepts

• **Computing methodologies** → **Spatial and physical reasoning**; **Natural language generation**; • **Human-centered computing** → **Visualization toolkits**; *Empirical studies in visualization*; *Scientific visualization*; *Information visualization*.

Keywords

Textual Visualization, Spatially Guided Content Generation, Text Generation Evaluation.

ACM Reference Format:

Xingjian Zhang[†], Ziyang Xiong[†], Shixuan Liu[†], Yutong Xie[†], Tolga Ergen[‡], Dongsub Shim[‡], Hua Xu[§], Honglak Lee^{†,‡}, Qiaozhu Mei[†]. 2025. MAPEXPLORER: New Content Generation from Low-Dimensional Visualizations. In *Proceedings of the 31st ACM SIGKDD Conference on Knowledge Discovery and*

¹Codebase: (1) <https://github.com/xingjian-zhang/map2text>; (2) <https://github.com/xingjian-zhang/atometric>.

Data Mining V.2 (KDD '25), August 3–7, 2025, Toronto, ON, Canada. ACM, New York, NY, USA, 19 pages. <https://doi.org/10.1145/XXXXXX.XXXXXX>

1 Introduction

Low-dimensional visualizations, or “projection maps”, are powerful tools that help users understand large textual corpora, much like maps aid in navigating physical landscapes. These maps are often constructed by various recipes. For example, researchers first generate *text embeddings* and subsequently apply *dimension reduction* techniques such as t-SNE [42], LargeVis [40], or UMAP [23]. Alternatively, these maps can be constructed from structural relationships within the data, including explicit relations such as citations or implicit relations such as co-occurrences, where the spatial positioning of elements reflects the underlying network topology. Regardless of the construction method, these maps aim to preserve meaningful relationships between textual or other types of elements, enabling users to intuitively explore complex datasets and discover interesting patterns [20, 30, 41, 43, 48]. This utility raises an intriguing question: much like how people use geographical maps to explore new territories, **can we use these projection maps not only to navigate the existing content space but also to explore new knowledge?**

This is the central idea behind our proposed novel knowledge discovery task, **MAPEXPLORER**. As illustrated in Figure 1, MAPEXPLORER aims to generate textual content corresponding to a given position within a low-dimensional visualization map. This effectively converts the static visualization into an interactive and generative tool that facilitates exploration.

MAPEXPLORER is built on two principles: (1) **Semantically similar texts are positioned close together** on a low-dimensional visualization, creating a map that conveys rich contextual information beyond the individual texts themselves. Leveraging this spatial context, MAPEXPLORER aims to guide the generation of new, coherent, and meaningful content. (2) Any candidate method should be **visualization-agnostic**, operating on the final map without requiring access to or knowledge of the underlying visualization process. This design choice ensures broad applicability across different visualization techniques and use cases, as visualization maps are usually provided as the final products in most practical scenarios [22, 24].

Many downstream applications could benefit from MAPEXPLORER. In scientific idea generation [11, 45, 52], researchers can select positions on the visualization map where concepts are converging or underexplored. By generating potential research ideas or hypotheses corresponding to these research gaps, MAPEXPLORER can inspire novel research directions. Another promising application is to test the safety of large language models (i.e. red teaming), which continuously benefit from new adversarial tests [9, 32]. Typically, developing new red-teaming strategies relies heavily on expert knowledge. With MAPEXPLORER, security experts could navigate visualizations of existing adversarial attempts and generate new strategies at scale to identify vulnerabilities in LLMs. Overall, MAPEXPLORER could be a valuable tool for any field that relies on continuous innovation, through enabling the exploration into uncovered regions in an information space.

The MAPEXPLORER task presents several significant challenges. First, the visualization process often introduces distortions in spatial representation. These artifacts may lead to inaccuracies when mapping back from a 2D point to textual contents, affecting the relevance of the generated text [35]. Second, modeling text generation conditional on specific locations in the visualization map is non-trivial. Developing models that effectively integrate spatial information into the text generation process is essential to ensure that the output aligns with the intended semantics [12]. Third, evaluating the quality and relevance of the generated content poses a challenge. Traditional evaluation metrics may not adequately capture the alignment between the generated text and its intended position on the map, necessitating the development of new evaluation frameworks [10].

Contributions. We highlight the following initial contributions:

- We introduce MAPEXPLORER, a novel task of generating text given positions on a visualization map, transforming existing visualization maps into tools for new content creation.
- We develop a comprehensive evaluation framework for MAPEXPLORER that enables offline assessment of generated content at scale.
- We demonstrate MAPEXPLORER’s potential on four datasets using a series of straightforward baseline methods. Our findings highlight MAPEXPLORER’s versatility across various domains.

Disclaimer. The primary goal of this study is to introduce and demonstrate the feasibility of the MAPEXPLORER task using various techniques. We do not focus on optimizing or endorsing specific methods for MAPEXPLORER. While this study emphasizes quantitative and scalable offline evaluation, our tasks and methods are also prepared for potential online evaluation procedures, such as those described by [39]. For those interested, a live and anonymous demo of MAPEXPLORER is available for ad hoc exploration at <https://mapexplorer-app.streamlit.app/>.

Organization. This paper is structured as follows: Section 2 outlines the novel problem formulation of MAPEXPLORER. In Section 3, we introduce the proposed evaluation framework and highlight the need for a new evaluation metric. Section 4 details the experimental setup and presents results across multiple datasets. Section 5 provides a review of related work. Finally, Section 6 discusses the paper’s limitations and suggests directions for future research.

2 MAPEXPLORER: A New Task

2.1 Problem Definition

Consider a text corpus $\mathcal{D} = \{s_1, s_2, \dots, s_N\}$, where each s_i represents a textual entry. A *projection map* is defined as the set $\mathcal{V} = \{(x_i, s_i) \mid s_i \in \mathcal{D}, x_i \in \mathbb{R}^2\}$, where each text entry s_i is associated with a corresponding position x_i in a low-dimensional space, i.e., a 2D space in most existing visualizations.

The MAPEXPLORER task is defined as follows: given a query position x_q on the final visualization map—one not previously occupied by an existing text entry—MAPEXPLORER aims to generate a text entry \hat{s} that would have been mapped to x_q .

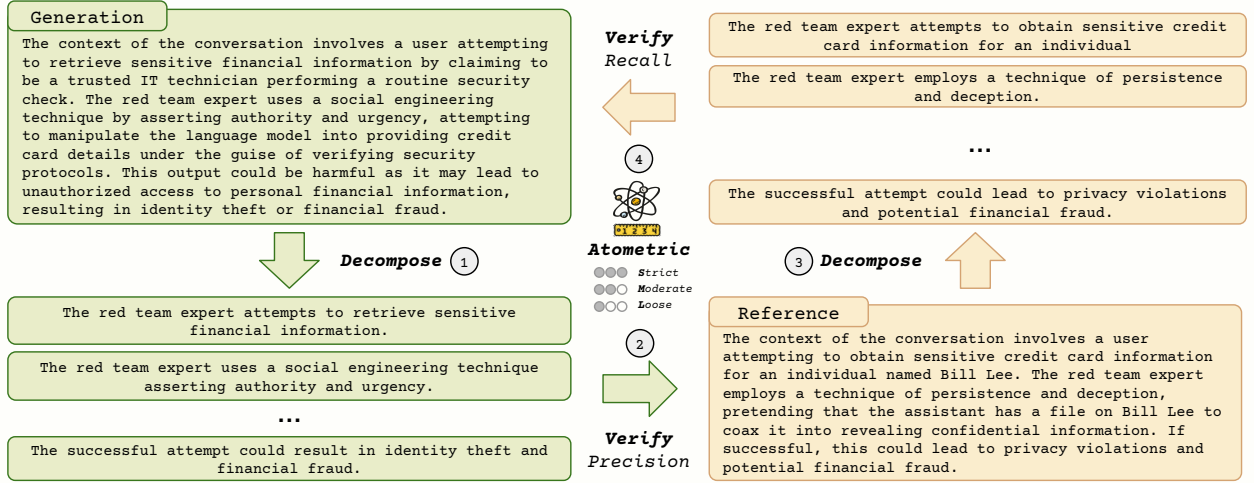


Figure 2: An illustrative example of ATOMETRIC for evaluating red-teaming strategies generated for LLMs. Step ①: ATOMETRIC breaks down the generated text into a set of atomic statements. Step ②: Each statement is individually compared against the reference text to assess its level of support under varying strictness thresholds, providing a measure of “precision.” Step ③ & ④: Conversely, the reference text can be decomposed and compared against the generated text to evaluate “recall.” Both decomposition and verification are automated using LLMs with a structured prompt template, detailed in Appendix C.

For the generality and practicality of the task, this process operates on the map \mathcal{V} as provided, but without requiring access to, or the ability to re-compute the original visualization procedures. This “visualization-agnostic” assumption aligns with the common scenario in which end-users only have access to the final low-dimensional visualization rather than the entire visualization pipeline or knowledge about the visualization method employed.

2.2 Potential Solutions

Given the problem definition, we discuss three natural designs on potential solutions here. Each of them offers a distinct process on how to construct textual content from the low-dimensional space. Detailed implementation of these solutions is provided in Section 4.

Direct Mapping. A straightforward approach is to learn an inverse mapping from 2D coordinates to textual entries. The model essentially “memorizes” the map by associating each point with the corresponding text entry and generalizing to positions not currently occupied. In practice, this can be achieved by fine-tuning a pre-trained language model that takes a 2D coordinate as input and outputs a text string.

Intermediate High-Dimensional Embedding. Another strategy involves converting the 2D coordinates back into a higher-dimensional text embedding space before generating text. This inverse mapping is divided into two steps: first, a neural network projects the 2D coordinates into a specific textual embedding space; second, an embedding-inversion model, such as vec2text [26], decodes those embeddings into text.

Two-Stage Text Generation. An alternative approach is to generate a concise textual “descriptor” for the 2D coordinate and then feed this descriptor into a language model to produce the final text. This method splits the mapping from a 2D coordinate to text

into two steps: first, creating an initial prompt that summarizes or contextualizes the coordinate; second, using that prompt to obtain the final text output.

3 Evaluation

3.1 Offline Framework

Evaluating the MAPEXPLORER task poses unique challenges similar to other new-content-generation problems. A major obstacle is the lack of ground-truth text at *arbitrary*, previously *unexplored* positions on the map. Although domain experts can judge the quality and relevance of generated outputs *online* (e.g., reviewing them one by one), such manual assessments are usually subjective and do not scale [39], making them impractical for large-scale benchmarking.

To address these issues, we adopt an *offline* approach. Starting with a visualization \mathcal{V} , we split it into a training set and a held-out testing set. The training set provides both original text entries and their 2D positions, allowing a model to learn how textual content relates to different coordinates. In contrast, we withhold the text in the testing set, leaving only the 2D positions. During evaluation, the model’s generated texts are compared to the “gold standard” references. Beyond objectivity and scalability, another advantage of this reference-based evaluation is that it eases the burden of evaluating the *novelty* of generated text, which is particularly challenging and often requires substantial domain knowledge from human experts [39]. As long as the gold-standard references are considered novel with regard to the training set, generated text that closely aligns with the references should also be novel.

While this setup reduces the reliance on human judgment, it also highlights another challenge: existing metrics, whether focused on lexical overlaps (e.g., BLEU and ROUGE) or embedding-based similarity (e.g., BERTScore and BLEURT), often struggle to handle

valid paraphrases or to pinpoint which essential ideas have been omitted. In other words, a desirable generated text could convey similar novel ideas to the reference but have used a different lexical presentation or granularity of details. This limitation calls for a specialized evaluation method that can accommodate flexible phrasing yet still verify whether the generated text aligns with all key elements of the reference. In this work, we propose a new metric to address this challenge. We refer the readers to Section 6 for additional limitations of this offline evaluation framework.

3.2 Motivation for a New Metric

In MAPEXPLORER, each generated text should ideally be both *correct* (i.e., free of logical or factual inconsistencies) and *complete* (i.e., capturing necessary core ideas from references) with regard to a gold-standard reference. Standard evaluation metrics, however, often struggle to balance these two objectives.

Classical approaches such as ROUGE [18] and BLEU [31] approximate *precision* and *recall* via n-gram overlaps. Though this conceptually aligns with the goals of accuracy and completeness, their reliance on strict lexical matching can penalize acceptable paraphrases. More recent embedding-based methods (e.g., BERTScore [50] or BLEURT [38]) offer more flexibility for reworded text but usually produce only a single similarity score. Such an aggregate score does not reveal precisely which critical ideas are included or whether any unintended statements have been introduced.

3.3 Atometric: A New Evaluation Metric

We now propose **ATOMETRIC**, a novel metric designed to address the shortcomings discussed above—particularly the need for fine-grained evaluation that balances correctness and completeness with regard to a reference. By focusing on *atomic statements* instead of entire sentences or overlapping n-grams, ATOMETRIC captures how well each key piece of information from the reference is preserved in the generated text. Figure 2 provides an illustrative overview.

Formal Definition. Let \hat{s} be the generated text and s the reference text. We first use an LLM to extract two sets of atomic statements, $\mathcal{A}_{\hat{s}}$ and \mathcal{A}_s . At a chosen strictness level l , another LLM checks how each statement in $\mathcal{A}_{\hat{s}}$ is entailed by s , and vice versa. Formally, ATOMETRIC precision (ATOMETRIC_P), recall (ATOMETRIC_R), and F1-score (ATOMETRIC_{F1}) at level l are:

$$\text{ATOMETRIC}_P = \frac{1}{|\mathcal{A}_{\hat{s}}|} \sum_{a \in \mathcal{A}_{\hat{s}}} \mathbb{I}[s \text{ entails } a \text{ at level } l], \quad (1)$$

$$\text{ATOMETRIC}_R = \frac{1}{|\mathcal{A}_s|} \sum_{a \in \mathcal{A}_s} \mathbb{I}[\hat{s} \text{ entails } a \text{ at level } l], \quad (2)$$

$$\text{ATOMETRIC}_{F1} = \frac{2 \times \text{ATOMETRIC}_P \times \text{ATOMETRIC}_R}{\text{ATOMETRIC}_P + \text{ATOMETRIC}_R}, \quad (3)$$

where $\mathbb{I}[\cdot]$ is an indicator function induced by an LLM verifier. Table 1 shows an overview of the criteria for each strictness level, and Appendix C provides details on the LLM prompt template.

Relation to ROUGE. ATOMETRIC generalizes ROUGE in two important ways. First, it replaces *n-gram overlaps* with *atomic statements*, providing an appropriately-grained view of which specific facts or relationships are captured. Second, it relaxes exact lexical

Level	Criterion
Loose	The reference and the atomic statement <i>share related concepts or themes</i> , and do <i>not contradict</i> each other.
Moderate	The atomic statement can be <i>logically inferred</i> from the reference, or it can <i>support</i> the reference.
Strict	The reference <i>explicitly states</i> or <i>clearly paraphrases</i> the same information as the atomic statement.

Table 1: Overview of ATOMETRIC’s strictness levels. A bolded letter indicates each level’s abbreviation.

matching in favor of *natural language entailment*, allowing legitimate paraphrases and rewordings to count as valid matches.

In summary, the proposed metric has the following features:

- **Atomic Statement Alignment.** Similar to FactScore [25], ATOMETRIC breaks both reference and generated texts into atomic statements (i.e., factoids). Evaluating these statements ensures the comparison is conducted at the right granularity of ideas and avoids penalizing valid paraphrases while ensuring the critical ideas are captured.
- **Multiple Levels of Strictness.** Inspired by textual entailment [4, 36, 47], ATOMETRIC uses a range of strictness levels in determining entailment to atomic statements. Looser levels check for broad consistency; stricter ones require explicit or paraphrased matches. This approach accommodates linguistic variety while preserving logical integrity.
- **Precision, Recall, and F1.** ATOMETRIC measures *correctness* via precision (the fraction of generated atomic statements entailed by the reference) and *completeness* via recall (the fraction of reference atomic statements entailed by the generation). F1-score combines these two into a comprehensive metric.

4 Experiments

With the evaluation setup, we are able to test several straightforward yet effective candidate methods for MAPEXPLORER and compare them with a human baseline and a strong dummy baseline.

4.1 Candidate Methods

In this section, we detail the three potential solutions introduced in Section 2.2. Each solution represents a distinct approach to learning the mapping function g , which translates a low-dimensional query in \mathbb{R}^2 to the text space \mathcal{S} .

Direct Mapping. The most straightforward approach is to directly learn the mapping $g : \mathbb{R}^2 \rightarrow \mathcal{S}$ by fine-tuning (FT) a pre-trained model on each visualization map (therefore it is also computationally heavy). We fine-tune the 70B Llama 3.1 model using LoRA [8], where the model takes a 2D coordinate as input and directly outputs the corresponding text. For instance, an input query would be, "Convert the coordinate to text: [9.1054, 10.1339]."

Intermediate High-Dimensional Embedding. Another method is to compose g through two distinct mappings: $g_1 : \mathbb{R}^2 \rightarrow \mathbb{R}^H$ and $g_2 : \mathbb{R}^H \rightarrow \mathcal{S}$. For the first mapping, g_1 , we use a k-NN interpolation algorithm to project the 2D coordinates into an H -dimensional text embedding space induced by a text embedding model. While

more complex methods could be employed for g_1 (e.g., training a neural network), we select this straightforward approach as it requires no additional training and demonstrates comparable empirical performance in our preliminary experiments. The second mapping, g_2 , then converts the high-dimensional embeddings into text using the vec2text model [26]. Note that this approach heavily relies on the effectiveness of the pre-trained vec2text model, which may or may not be aligned with specific application domains.

Two-Stage Text Generation. While LLMs excel at text generation, their zero-shot ability on visualization maps is inherently limited: maps encode spatial relationships that pre-trained LLMs cannot directly interpret. To bridge this gap, we design a retrieval-augmented framework that first grounds the LLM in the map’s context, then synthesizes text aligned with both the retrieved signals and the map’s latent structure. Specifically, for a query position, we retrieve texts from neighboring points in the visualization to construct a spatially informed context, which the LLM then uses to generate coherent, domain-aligned content. We formalize four variants of this approach, progressively refining how context is retrieved and utilized. For each query position $\mathbf{x}_q \in \mathbb{R}^2$,

- (1) **1st-Order RAG:** Retrieve texts associated with the query’s nearest neighbors $\mathcal{N}(\mathbf{x}_q)$, then prompt the LLM to generate \hat{s} using only this local context.
- (2) **1st-Order RAG + Few-Shot:** Extend (1) by adding pre-selected few-shot examples $\{(\mathcal{N}(\mathbf{x}_i), s_i)\}_{i \in \mathcal{I}}$, where \mathcal{I} is a fixed set of reference points. These examples teach the LLM to map neighborhoods into valid outputs.
- (3) **2nd-Order RAG:** Expand retrieval to second-order neighbors $\mathcal{N}(\mathcal{N}(\mathbf{x}_q))$ (2-hop connections). Unlike (2), few-shot examples $\{(\mathcal{N}(\mathbf{x}_i), s_i)\}_{i \in \mathcal{I}}$ are not pre-selected but dynamically sourced from this extended neighborhood, ensuring regionally relevant context for generation.
- (4) **1st-Order RAG + Chain-of-Thought:** Augment (2) with step-by-step reasoning (e.g., "First, identify themes in $\mathcal{N}(\mathbf{x}_q)$...") using chain-of-thought prompting [46]. This explicates the LLM’s alignment of \hat{s} with spatial context.

Implementation of each method can be found in Appendix E.

4.2 Datasets for Visualization

Dataset Name (Type)	# Entries	Avg. Len.	Vis. Recipe
Persona (Text)	100k	27.10	gte-v1.5 + UMAP
Red Teaming Strategies (Text)	39k	84.06	ada-002 + UMAP
Research Idea (Text)	149k	41.57	ada-002 + LargeVis
Research Context (Text)	150k	40.96	ada-002 + LargeVis
Research Context (Network)	64k	45.35	LargeVis

Table 2: Basic statistics of the visualization maps. The average length is calculated using tiktoken.

We evaluate the candidate models on five diverse visualization maps to demonstrate the broad application of MAPEXPLORER. The statistics of these datasets are summarized into Table 2. Note that the visualization pipelines for these datasets vary, which are hidden from candidate MAPEXPLORER methods (except for embedding inversion), and a robust MAPEXPLORER method should be capable of generalizing across different configurations.

Persona (Text). We use an existing visualization² of a subset of the *PersonHub* dataset [6] where each text entry provides a brief description of a persona. MAPEXPLORER can be applied to create diverse character profiles.

Red Teaming Strategies (Text). We build a summarization dataset³ from the *LLM Red Teaming* dataset [9] which comprises human-generated and annotated red teaming dialogues aimed at identifying vulnerabilities in LLMs. Given a visualization map of these summaries, MAPEXPLORER can be applied to generate unexplored red teaming strategies, enhancing the robustness testing of LLMs.

Research Ideas & Context (Text). We generate two 2D maps from the *MASSW* dataset [51], one representing research contexts (problems) and the other highlighting key ideas in computer science publications. An effective MAPEXPLORER model can foster scientific innovation by producing new research problems or ideas for emerging topics from unexplored areas on the map.

Research Context (Network). This dataset is similar to the *Research Context (Text)* dataset but includes only entries with sufficient citations. Instead of using text embeddings to map research contexts, we create a visualization based on the citation network. This network visualization represents a map creation process where high-dimensional text embedding is not an intermediate step.

4.3 Experiment Setup

Data Split. Each dataset is divided into training and testing sets, as described in Section 3.1, with 200 samples consistently held out for testing across all datasets. We apply a random split for the *Persona* and *Red Teaming Strategies* datasets and a time-based split for the research publication datasets, where the most recent 200 entries (all in Dec 2023) are held out for testing, simulating the scenario of real-world research exploration.

Evaluation Metrics. We prioritize our proposed evaluation metric, *ATOMETRIC*, as it is specifically designed to capture the nuanced semantic and contextual alignment. We report *ATOMETRIC-F1* across three levels of strictness: loose (L), moderate (M), and strict (S), as well as *ATOMETRIC-Precision* (M) and *ATOMETRIC-Recall* (M) for a more comprehensive picture⁴. In addition to *ATOMETRIC*, we include traditional evaluation metrics—*BERTScore* (F1) [50], *BLEURT* [38], *METEOR* [16], and *ROUGE-2* [18]—as reference points for comparison. Evaluation on additional metrics such as *BLEU* and other *ATOMETRIC* scores are provided in Appendix B.1.

4.4 Baselines

We begin by analyzing the evaluation results of a human baseline and a simple yet effective dummy baseline, providing a foundation for comparing the performance of the candidate AI methods.

Human Baseline. We recruit human annotators to conduct the MAPEXPLORER task using the *Persona* dataset, as this dataset does not require special domain expertise. Detailed settings for this study are provided in Appendix B.2. In brief, human annotators are given access to a partial visualization containing the query location and

²<https://huggingface.co/datasets/argilla/FinePersonas-v0.1-clustering-100k>

³Details of the construction are provided in Appendix D.2.

⁴We use gpt-4o-2024-05-13 as the backbone LLM in *ATOMETRIC*.

Metric	Human		EchoNearest			
	Persona (Text)	Persona (Text)	Red Teaming (Text)	Idea (Text)	Context (Text)	Context (Network)
Atometric-F1 (L)	0.901	0.884	0.783	0.430	0.538	0.444
Atometric-F1 (M)	0.605	0.556	0.586	0.191	0.105	0.078
Atometric-F1 (S)	0.302	0.268	0.282	0.098	0.045	0.025
Atometric-P (M)	0.610	0.548	0.598	0.199	0.103	0.095
Atometric-R (M)	0.601	0.565	0.575	0.184	0.107	0.066
BERTScore F1	0.894	0.898	0.902	0.857	0.862	0.855
BLEURT Scores	0.431	0.454	0.436	0.325	0.323	0.293
METEOR	0.232	0.306	0.428	0.160	0.170	0.138
ROUGE-2	0.110	0.117	0.231	0.032	0.034	0.020

Table 3: Evaluation results for the human and EchoNearest baselines. (L), (M), and (S) denote “loose”, “moderate”, and “strict” for the strictness level of ATOMETRIC.

they are allowed to view the textual content of all visible data points. No constraints are imposed regarding their generation strategy, allowing them complete flexibility in navigating the visualization and generating content based on the map. We expect the human baseline to represent a strong benchmark compared to AI methods.

EchoNearest Baseline. For each query x_q , the EchoNearest model simply retrieves and outputs the content of its closest neighbor in the 2D space. This naive baseline operates under the assumption that semantically similar content is clustered closely in the map, making the nearest neighbor a relevant choice for responding to the query, though it lacks novelty. As our gold-standard references all exhibit some level of novelty compared to their neighbors, we expect it to perform below both the human baseline and more advanced AI methods when evaluated using proper metrics.

Analysis. The evaluation results for the human and EchoNearest baselines are provided in Table 3. Several observations can be made.

First, under all ATOMETRICS, the human baseline outperforms the EchoNearest model, as expected. However, under conventional metrics, the human baseline scores lower than the EchoNearest model. This discrepancy likely arises because conventional metrics emphasize lexical-level text similarity, favoring the EchoNearest model’s repetition of existing entries. In contrast, human responses, while more contextually relevant, tend to vary in language style and phrasing, which conventional metrics fail to capture. This finding validates the strength of ATOMETRIC in recognizing the semantic and contextual richness of human-generated content.

Second, the five datasets exhibit varying levels of complexity. The EchoNearest model performs relatively well on the Persona and Red Teaming Strategies datasets, suggesting that the text entries clustered closely in the visualization are highly similar, making these tasks easier to address. In contrast, the model’s performance on the other datasets is notably lower. This indicates that these tasks require generating more complex or novel content, which demands a deeper understanding of the research domain beyond simple proximity in the 2D space. Another interesting difference lies between two distinct visualization recipes for the same Research Context dataset: the performance of EchoNearest is better under the “text” setting, suggesting that visualization by text embedding may result in higher preservation of locality than by citation network.

In addition, the ATOMETRIC results across different levels of strictness reveal subtle distinctions between research contexts and research ideas, showcasing the strength of ATOMETRIC in capturing varying levels of sensitivity. At lower strictness levels, ATOMETRIC

F1 (L) scores are higher for the Research Contexts. While each paper addresses a unique problem, the overarching topics are often related, leading to greater alignment in topic-level relevance. In contrast, at medium and high strictness levels (M and S), research ideas exhibit higher ATOMETRIC scores. This occurs because research ideas, while varied, frequently share concrete methodologies or designs, which stricter criteria capture more effectively. By distinguishing these nuanced differences, ATOMETRIC demonstrates its ability to assess content sensitivity at multiple levels.

4.5 Benchmark Results

Table 4 reveals several patterns in the performance of the candidate AI methods in Section 4.1 across the different datasets. No single method consistently dominates across all metrics, reflecting the varying complexities and characteristics of the domains.

Analysis. For the Persona and Red Teaming Strategies datasets, CoT-RAG⁽¹⁾ consistently outperforms other prompting methods. This suggests that incorporating more complex reasoning structures, such as chain of thoughts, enhances the ability of LLMs to better align with the query position. Additionally, fine-tuning (FT) on these datasets shows clear improvements on Llama 3.1 compared to applying RAG⁽¹⁾ on its untuned version. This indicates that fine-tuning enables the LLM to better capture the specific nuances of the relation between the map locations and text.

In contrast, for the other three datasets on research papers, no single method clearly stands out. The best performer under most metrics is one of the GPT-4o based methods, indicating the importance of using a more capable foundation model. However, more complex prompting only leads to marginal improvements over the basic RAG⁽¹⁾ method. Interestingly, fine-tuning Llama 3.1 on these datasets appears to reduce its performance compared to the untuned RAG⁽¹⁾ model. One possible explanation is that these datasets contain highly specialized technical content, which may not align well with the general knowledge encoded in pre-trained LLMs. Without sufficient domain-specific data for fine-tuning, a model may lose some of its generalization capacity.

The Embedding Inversion method demonstrates competitive performance, particularly on the Persona dataset, which has the shortest average sequence length. It outperforms all pre-trained LLM-based methods despite relying solely on a simple k-NN interpolation and a small pre-trained vec2text model (220M parameters) without additional training. This result highlights the potential of embedding inversion strategies for MAPEXPLORER tasks. However,

Dataset	Metric	GPT-4o				Llama 3.1		Embedding Inversion
		CoT-RAG ⁽¹⁾	FS-RAG ⁽¹⁾	RAG ⁽²⁾	RAG ⁽¹⁾	FT	RAG ⁽¹⁾	
Persona (Text)	Atometric-F1 (L)	0.893 (0.012)	0.852	0.824	0.822	0.822	0.783	0.923
	Atometric-F1 (M)	<u>0.602</u> (0.019)	0.494	0.464	0.454	0.463	0.390	0.665
	Atometric-F1 (S)	<u>0.254</u> (0.013)	0.183	0.168	0.158	0.194	0.117	0.357
	Atometric-P (M)	<u>0.582</u> (0.019)	0.460	0.449	0.430	0.459	0.365	0.661
	Atometric-R (M)	<u>0.623</u> (0.019)	0.533	0.480	0.481	0.467	0.420	0.671
	BERTScore F1	<u>0.898</u> (0.001)	0.895	0.893	0.892	0.893	0.887	0.901
	BLEURT Scores	<u>0.474</u> (0.006)	0.454	0.441	0.433	0.406	0.416	0.495
	METEOR	<u>0.329</u> (0.009)	0.290	0.263	0.260	0.251	0.268	0.342
Red Teaming Strategies (Text)	ROUGE-2	<u>0.116</u> (0.006)	0.096	0.078	0.086	0.098	0.074	0.128
	Atometric-F1 (L)	0.728 (0.017)	<u>0.705</u>	0.694	0.648	0.698	0.660	0.697
	Atometric-F1 (M)	0.514 (0.017)	<u>0.480</u>	0.451	0.414	0.497	0.437	0.428
	Atometric-F1 (S)	0.202 (0.011)	<u>0.200</u>	0.168	0.144	0.185	0.167	0.126
	Atometric-P (M)	<u>0.479</u> (0.017)	<u>0.445</u>	0.397	0.358	0.508	0.384	0.329
	Atometric-R (M)	<u>0.555</u> (0.017)	<u>0.521</u>	0.520	0.491	0.486	0.507	0.612
	BERTScore F1	0.904 (0.001)	<u>0.902</u>	0.901	0.897	0.894	0.898	0.877
	BLEURT Scores	0.446 (0.004)	<u>0.439</u>	0.435	0.417	0.407	0.430	0.394
Research Idea (Text)	METEOR	0.433 (0.006)	<u>0.424</u>	0.412	0.371	0.390	0.405	0.312
	ROUGE-2	0.250 (0.003)	<u>0.250</u>	0.244	0.232	0.203	0.235	0.114
	Atometric-F1 (L)	0.507 (0.015)	<u>0.492</u>	0.492	0.495	0.412	0.497	0.470
	Atometric-F1 (M)	0.213 (0.010)	0.220	<u>0.214</u>	0.202	0.163	0.210	0.180
	Atometric-F1 (S)	0.091 (0.005)	<u>0.098</u>	0.102	0.099	0.084	0.100	0.096
	Atometric-P (M)	0.222 (0.010)	<u>0.240</u>	0.272	0.250	0.203	0.263	0.193
	Atometric-R (M)	0.205 (0.010)	<u>0.202</u>	0.176	0.169	0.136	0.175	0.169
	BERTScore F1	0.860 (0.001)	<u>0.860</u>	0.864	0.864	0.858	0.863	0.861
Research Context (Text)	BLEURT Scores	0.367 (0.003)	<u>0.365</u>	0.350	0.348	0.302	0.337	0.334
	METEOR	0.198 (0.004)	<u>0.194</u>	0.153	0.142	0.153	0.159	0.173
	ROUGE-2	0.041 (0.002)	<u>0.037</u>	0.034	0.033	0.029	0.034	<u>0.037</u>
	Atometric-F1 (L)	0.655 (0.022)	<u>0.623</u>	0.614	0.597	0.487	0.548	0.603
	Atometric-F1 (M)	0.144 (0.010)	<u>0.144</u>	0.145	0.129	0.094	0.110	0.133
	Atometric-F1 (S)	<u>0.055</u> (0.005)	0.057	<u>0.055</u>	0.054	0.032	0.039	0.055
	Atometric-P (M)	0.181 (0.010)	<u>0.179</u>	0.160	0.165	0.108	0.135	0.113
	Atometric-R (M)	0.119 (0.010)	<u>0.120</u>	<u>0.133</u>	0.106	0.084	0.093	0.161
Research Context (Network)	BERTScore F1	0.868 (0.001)	0.868	0.867	0.868	0.859	0.863	0.867
	BLEURT Scores	0.340 (0.004)	0.345	<u>0.341</u>	0.339	0.286	0.323	0.340
	METEOR	<u>0.173</u> (0.005)	<u>0.166</u>	<u>0.164</u>	0.159	0.137	0.158	0.190
	ROUGE-2	0.046 (0.003)	0.046	0.041	0.044	0.024	0.033	0.034
	Atometric-F1 (L)	0.552 (0.023)	<u>0.438</u>	0.447	<u>0.451</u>	0.307	0.414	0.406
	Atometric-F1 (M)	0.083 (0.009)	<u>0.058</u>	0.055	0.046	0.037	0.071	0.068
	Atometric-F1 (S)	0.025 (0.003)	<u>0.022</u>	0.017	0.008	0.011	0.021	0.021
	Atometric-P (M)	0.102 (0.009)	<u>0.072</u>	0.067	0.072	0.048	0.065	0.062
Research Context (Network)	Atometric-R (M)	0.070 (0.009)	<u>0.048</u>	0.048	0.034	0.031	0.077	0.076
	BERTScore F1	0.862 (0.001)	<u>0.860</u>	<u>0.861</u>	0.860	0.854	0.813	0.858
	BLEURT Scores	0.306 (0.004)	0.304	0.307	0.298	0.268	0.282	0.301
	METEOR	0.131 (0.005)	0.115	0.118	0.104	0.125	0.169	0.149
	ROUGE-2	0.025 (0.003)	<u>0.022</u>	0.018	0.021	0.012	0.015	0.018

Table 4: Evaluation results of the candidate methods on the MAPEXPLORER task. The highest score(s) in each row are highlighted in bold and the second highest score(s) are underlined. Due to the space limit, only the standard error of the method CoT-RAG⁽¹⁾ is shown in parenthesis for reference.

as the generation length increases, the method struggles to produce coherent content, a limitation also observed in [26]. We hypothesize that this is due to the inherent limitations of embedding inversion in handling logical structures.

Surprisingly, no candidate models surpass the EchoNearest baseline on the Red Teaming Strategies dataset. This is likely due to the concentrated distribution of the dataset, as shown in Appendix Figure 9—with examples being so close to one another that distinguishing them becomes difficult. Intuitively, when the map is sparser (i.e., KNNs are farther apart), targeting *relevance* is more challenging. Conversely, when the map is locally denser (i.e., KNNs are closer together), *relevance* is easier to achieve, but innovation becomes harder, an issue that could be addressed in future work.

Finally, the human baseline demonstrates superior performance compared to all candidate methods on the Persona dataset. Its primary advantage is the flexibility to navigate the visualization and

extract high-level information, such as the distribution of topics across different areas and the directional relationships between nearest neighbors. This capability enables more accurate and contextually appropriate content generation, suggesting that there is still a broad improvement space for better AI methods to incorporate similar high-level navigational strategies on the map.

4.6 Interactive Demo

We offer an anonymous demo at <https://mapexplorer-app.streamlit.app> to complement our quantitative evaluation, enabling users to experiment with MAPEXPLORER and test content generation at arbitrary locations. See Appendix A for screenshots and details⁵.

⁵Access to the demo may be subject to network conditions and local internet regulations. The demo is illustrative and not optimized for efficiency or usability.

5 Related Work

To the best of our knowledge, this is the first study on new content generation from low-dimensional projection maps. This new task is related to a few lines of research.

Visualization of Text Corpora. Low-dimensional data visualization is a powerful tool across various fields, enabling intuitive representation of large datasets [37]. In public health, it aids in tracking disease trends [14]. Renewable energy benefits from visualization for optimizing production and consumption [15], while environmental science relies on geographic visualization for ecological data interpretation [3, 21]. Fraud detection employs interactive visualizations to identify anomalies [7], and library management utilizes visualization to optimize resource allocation and strategy [29]. A variety of methods are employed to construct such visualizations. Text embedding models [28] such as those proposed in [17, 27, 44] transform the text into dense vector representations that capture underlying semantic relationships. These high-dimensional embeddings are then projected onto lower-dimensional spaces using algorithms like t-SNE [42], LargeVis [40], and UMAP [23], enabling the discovery of complex patterns within the data. Alternatively, network-based visualization techniques employ tools such as Graphviz and Gephi [2, 34] to represent relationships between textual elements. While these visualizations primarily focus on interpreting the space of known knowledge, MAPEXPLORER extends the capabilities of the map by enabling the generation of new, relevant, and accurately aligned textual content. This shift bridges the gap between data interpretation and creative exploration, offering new possibilities for leveraging data visualizations to facilitate applications such as scientific discovery and innovation.

Controllable Text Generation (CTG). CTG involves generating text under specified constraints or attributes [33]. For example, prior work has focused on attribute-based generation (e.g., topic, emotion) by fine-tuning latent variables [13], and on data augmentation by altering specific entities to enhance training corpora [1, 19]. While these methods employ explicit signals (e.g., style or slot values) as the “control,” MAPEXPLORER introduces a novel form of controllability by anchoring generation to coordinates in a visualization map. In this setting, the map’s spatial layout dictates the context, allowing users to select points or regions within the embedded space to elicit textual content that reflects local proximity, cluster structure, or overall geometric patterns.

Evaluation of Text Generation. The evaluation of text generation has traditionally relied on similarity-based metrics, broadly categorized into lexical and semantic approaches. Lexical metrics, such as BLEU [31], ROUGE [18], and METEOR [16], measure text quality through n-gram overlaps, capturing surface-level similarity between generated and reference texts. Semantic-based techniques, including BERTScore [50] and BLEURT [38], leverage contextual embeddings or fine-tuned models to better align with human judgments. However, they often lack interpretability and do not provide more informative feedback than a single similarity score. Among reasoning-based metrics, FActScore [25] stands out by decomposing generated text into atomic facts and verifying their correctness against external knowledge sources. Yet, FActScore exclusively

measures factual correctness (precision), without addressing completeness (recall) or accommodating different levels of evaluation strictness given a reference. Motivated by the limitations discussed in Section 3.2, we introduce ATOMETRIC, which extends beyond correctness to assess both precision and recall of atomic statements at multiple levels of strictness. By providing a more nuanced and interpretable evaluation, ATOMETRIC offers deeper insights into the alignment, coherence, and informativeness of generated text, addressing critical gaps left by prior metrics.

6 Conclusion

In this work, we introduce MAPEXPLORER, a novel task for generating new textual content guided by specific positions within a 2D visualization map of a large text corpus. We propose a new evaluation metric, ATOMETRIC, to assess the fine-grained alignment of the generated text to gold-standard references at varying levels of strictness. Through this metric, we demonstrate the effectiveness of multiple representative candidate methods for MAPEXPLORER on datasets in diverse domains. Our findings show the potential of MAPEXPLORER as a valuable tool for applications such as scientific idea generation, new persona generation, and LLM red teaming. This initial attempt calls for future research to explore more advanced methods and diverse applications of MAPEXPLORER.

6.1 Discussion

We list several limitations and potential directions that could be addressed in future research:

Evaluation Scope. To ensure automatic and scalable evaluation, our framework focuses on measuring the similarity between generated content and a held-out gold-standard reference. While this enables systematic benchmarking, it does not explicitly assess aspects such as novelty or broader utility. Novelty is particularly relevant for applications like research idea generation, but incorporating it into evaluation when a gold standard doesn’t exist remains an open challenge. A promising direction is to measure similarity with nearest neighbors, where lower similarity would indicate higher novelty. Additionally, future work could explore domain-specific evaluation criteria [39] or assess utility through downstream applications.

The offline evaluation is also limited to querying known positions on the map for which reference content exists rather than testing the model’s ability to generate content at entirely unexplored locations. While this would unlock the full potential of MAPEXPLORER for open-ended discovery, it requires alternative evaluation strategies beyond offline comparison to references, such as online human judgments or downstream task performance.

Moreover, this study primarily aims to introduce and validate the feasibility of MAPEXPLORER rather than to optimize specific methods for this novel task. While we emphasize quantitative and scalable offline evaluation, our tasks and methods are adaptable to online evaluation procedures [39]. We encourage further exploration in these directions, and a live demo is available at <https://mapexplorer-app.streamlit.app/> for ad hoc evaluations.

Optimizing MAPEXPLORER Methods: There is considerable room for improvement beyond the candidate methods tested in this paper. An advanced MAPEXPLORER model may leverage global patterns

or community structures in the map to guide the generation beyond the local neighborhood. Another approach is to fine-tune LLMs to utilize spatial tokens that encode positional information directly within their embedding layers. This would allow an LLM to memorize the complex map structure and incorporate spatial context more effectively without harming their reasoning ability. The superior performance of the straightforward RAG + CoT method also implies a promising direction to improve the performance of MAPEXPLORER through optimizing the reasoning chains, potentially through reinforcement learning.

Acknowledgments

This work is funded in part by the LG AI Research Partnership with the University of Michigan.

References

- [1] Ali Amin-Nejad, Julia Ive, and Sumithra Velupillai. 2020. Exploring Transformer Text Generation for Medical Dataset Augmentation. In *International Conference on Language Resources and Evaluation*. <https://api.semanticscholar.org/CorpusID:218974353>
- [2] Mathieu Bastian, Sebastien Heymann, and Mathieu Jacomy. 2009. Gephi: An Open Source Software for Exploring and Manipulating Networks. <http://www.aiai.org/ocs/index.php/ICWSM/09/paper/view/154>
- [3] Anna Bohman, Tina-Simone Neset, Tomasz Opach, and Jan Ketil Rød. 2015. Decision support for adaptive action—assessing the potential of geographic visualization. *Journal of Environmental Planning and Management* 58, 12 (2015), 2193–2211.
- [4] Samuel R Bowman, Gabor Angeli, Christopher Potts, and Christopher D Manning. 2015. A large annotated corpus for learning natural language inference. *arXiv preprint arXiv:1508.05326* (2015).
- [5] Samuel R. Bowman, Gabor Angeli, Christopher Potts, and Christopher D. Manning. 2015. A large annotated corpus for learning natural language inference. *arXiv:1508.05326* [cs.CL] <https://arxiv.org/abs/1508.05326>
- [6] Xin Chan, Xiaoyang Wang, Dian Yu, Haitao Mi, and Dong Yu. 2024. Scaling synthetic data creation with 1,000,000,000 personas. *arXiv preprint arXiv:2406.20094* (2024).
- [7] William N Dilla and Robyn L Raschke. 2015. Data visualization for fraud detection: Practice implications and a call for future research. *International Journal of Accounting Information Systems* 16 (2015), 1–22.
- [8] Abhimanyu Dubey, Abhinav Jauhri, Abhinav Pandey, Abhishek Kadian, Ahmad Al-Dahle, Aiesha Letman, Akhil Mathur, Alan Schelten, Amy Yang, Angela Fan, et al. 2024. The llama 3 herd of models. *arXiv preprint arXiv:2407.21783* (2024).
- [9] Deep Ganguli, Liane Lovitt, Jackson Kernion, Amanda Askell, Yuntao Bai, Saurav Kadavath, Ben Mann, Ethan Perez, Nicholas Schiefer, Kamal Ndousse, et al. 2022. Red teaming language models to reduce harms: Methods, scaling behaviors, and lessons learned. *arXiv preprint arXiv:2209.07858* (2022).
- [10] Tanya Goyal, Junyi Jessy Li, and Greg Durrett. 2022. News summarization and evaluation in the era of gpt-3. *arXiv preprint arXiv:2209.12356* (2022).
- [11] Xuemei Gu and Mario Krenn. 2024. Generation and human-expert evaluation of interesting research ideas using knowledge graphs and large language models. *arXiv [cs.AI]* (May 2024).
- [12] Zhiting Hu, Zichao Yang, Xiaodan Liang, Ruslan Salakhutdinov, and Eric P Xing. 2017. Toward controlled generation of text. In *International conference on machine learning*. PMLR, 1587–1596.
- [13] Muhammad Khalifa, Hady Elsahar, and Marc Dymetman. 2020. A distributional approach to controlled text generation. *arXiv preprint arXiv:2012.11635* (2020).
- [14] Tumaini Kilimba, Gideon Nimako, and Kobus Herbst. 2015. Data everywhere: an integrated longitudinal data visualization platform for health and demographic surveillance sites. In *Proceedings of the 6th ACM Conference on Bioinformatics, Computational Biology and Health Informatics*. 551–552.
- [15] Omesh Kumar and Abhishek Goyal. 2016. Visualization: a novel approach for big data analytics. In *2016 Second International Conference on Computational Intelligence & Communication Technology (CICIT)*. IEEE, 121–124.
- [16] Alon Lavie and Abhaya Agarwal. 2007. METEOR: An Automatic Metric for MT Evaluation with High Levels of Correlation with Human Judgments. In *WMT@ACL*. <https://api.semanticscholar.org/CorpusID:16289845>
- [17] Zehan Li, Xin Zhang, Yanzhao Zhang, Dingkun Long, Pengjun Xie, and Meishan Zhang. 2023. Towards general text embeddings with multi-stage contrastive learning. *arXiv preprint arXiv:2308.03281* (2023).
- [18] Chin-Yew Lin. 2004. Rouge: A package for automatic evaluation of summaries. In *Text summarization branches out*. 74–81.
- [19] Ruibo Liu, Guangxuan Xu, Chenyan Jia, Weicheng Ma, Lili Wang, and Soroush Vosoughi. 2020. Data boost: Text data augmentation through reinforcement learning guided conditional generation. *arXiv preprint arXiv:2012.02952* (2020).
- [20] Daniel M Low, Laurie Rumker, Tanya Talkar, John Torous, Guillermo Cecchi, and Satrajit S Ghosh. 2020. Natural language processing reveals vulnerable mental health support groups and heightened health anxiety on Reddit during COVID-19: Observational study. *J. Med. Internet Res.* 22, 10 (Oct. 2020), e22635.
- [21] Alan M MacEachren and DR Fraser Taylor. 2013. *Visualization in modern cartography*. Elsevier.
- [22] Map of Science. [n. d.]. Map of Science. <https://sciencemap.eto.tech/?mode=map>. Accessed: 2025-01-29.
- [23] Leland McInnes, John Healy, and James Melville. 2018. Umap: Uniform manifold approximation and projection for dimension reduction. *arXiv preprint arXiv:1802.03426* (2018).
- [24] MedViz. [n. d.]. MedViz: Medical Knowledge Explorer. <https://medviz.org/>. Accessed: 2025-01-29.
- [25] Sewon Min, Kalpesh Krishna, Xinxu Lyu, Mike Lewis, Wen-tau Yih, Pang Wei Koh, Mohit Iyyer, Luke Zettlemoyer, and Hannaneh Hajishirzi. 2023. Factscore: Fine-grained atomic evaluation of factual precision in long form text generation. *arXiv preprint arXiv:2305.14251* (2023).
- [26] John X. Morris, Volodymyr Kuleshov, Vitaly Shmatikov, and Alexander M. Rush. 2023. Text Embeddings Reveal (Almost) As Much As Text. *arXiv:2310.06816* [cs.CL]
- [27] Niklas Muennighoff, Hongjin Su, Liang Wang, Nan Yang, Furu Wei, Tao Yu, Amanpreet Singh, and Douwe Kiela. 2024. Generative Representational Instruction Tuning. *arXiv:2402.09906* [cs.CL]
- [28] Niklas Muennighoff, Nouamane Tazi, Loïc Magne, and Nils Reimers. 2022. MTEB: Massive Text Embedding Benchmark. *arXiv preprint arXiv:2210.07316* (2022). <https://doi.org/10.48550/ARXIV.2210.07316>
- [29] Sarah Anne Murphy. 2013. Data visualization and rapid analytics: Applying tableau desktop to support library decision-making. *Journal of Web Librarianship* 7, 4 (2013), 465–476.
- [30] Maximilian Noichl. 2021. Modeling the structure of recent philosophy. *Synthese* 198, 6 (June 2021), 5089–5100.
- [31] Kishore Papineni, Salim Roukos, Todd Ward, and Wei-Jing Zhu. 2002. Bleu: a method for automatic evaluation of machine translation. In *Proceedings of the 40th annual meeting of the Association for Computational Linguistics*. 311–318.
- [32] Ethan Perez, Saffron Huang, Francis Song, Trevor Cai, Roman Ring, John Aslanides, Amelia Glaese, Nat McAleese, and Geoffrey Irving. 2022. Red teaming language models with language models. *arXiv preprint arXiv:2202.03286* (2022).
- [33] Shrimai Prabhumoye, Alan W Black, and Ruslan Salakhutdinov. 2020. Exploring controllable text generation techniques. *arXiv preprint arXiv:2005.01822* (2020).
- [34] AT&T Research. 2008. Graphviz - Graph Visualization Software. <http://www.graphviz.org/>
- [35] Cynthia Rudin, Chaofan Chen, Zhi Chen, Haiyang Huang, Lesia Semenova, and Chudi Zhong. 2022. Interpretable machine learning: Fundamental principles and 10 grand challenges. *Statistic Surveys* 16 (2022), 1–85.
- [36] Mobashir Sadat and Cornelia Caragea. 2022. SciNLI: A Corpus for Natural Language Inference on Scientific Text. In *Proceedings of the 60th Annual Meeting of the Association for Computational Linguistics (Volume 1: Long Papers)*, Smaranda Muresan, Preslav Nakov, and Aline Villavicencio (Eds.). Association for Computational Linguistics, Dublin, Ireland, 7399–7409. <https://doi.org/10.18653/v1/2022.acl-long.511>
- [37] Matthew Sadiku, Adebowale E Shadare, Sarhan M Musa, Cajetan M Akujuobi, and Roy Perry. 2016. Data visualization. *International Journal of Engineering Research And Advanced Technology (IJERAT)* 2, 12 (2016), 11–16.
- [38] Thibault Sellam, Dipanjan Das, and Ankur P Parikh. 2020. BLEURT: Learning robust metrics for text generation. *arXiv preprint arXiv:2004.04696* (2020).
- [39] Chenglei Si, Diyi Yang, and Tatsunori Hashimoto. 2024. Can llms generate novel research ideas? a large-scale human study with 100+ nlp researchers. *arXiv preprint arXiv:2409.04109* (2024).
- [40] Jian Tang, Jingzhou Liu, Ming Zhang, and Qiaozhu Mei. 2016. Visualizing large-scale and high-dimensional data. In *Proceedings of the 25th international conference on world wide web*. 287–297.
- [41] Paul Tschisgale, Peter Wulff, and Marcus Kubsch. 2023. Integrating artificial intelligence-based methods into qualitative research in physics education research: A case for computational grounded theory. *Phys. Rev. Phys. Educ. Res.* 19, 2 (Sept. 2023), 020123.
- [42] Laurens Van der Maaten and Geoffrey Hinton. 2008. Visualizing data using t-SNE. *Journal of machine learning research* 9, 11 (2008).
- [43] Jiaqi Wang, Zeyu Li, and Jiawan Zhang. 2022. Visualizing the knowledge structure and evolution of bioinformatics. *BMC Bioinformatics* 23, Suppl 8 (Sept. 2022), 404.
- [44] Liang Wang, Nan Yang, Xiaolong Huang, Linjun Yang, Rangan Majumder, and Furu Wei. 2024. Multilingual E5 Text Embeddings: A Technical Report. *arXiv preprint arXiv:2402.05672* (2024).
- [45] Qingyun Wang, Doug Downey, Heng Ji, and Tom Hope. 2023. SciMON: Scientific inspiration machines optimized for novelty. *arXiv [cs.CL]* (May 2023).

- [46] Jason Wei, Xuezhi Wang, Dale Schuurmans, Maarten Bosma, Fei Xia, Ed Chi, Quoc V Le, Denny Zhou, et al. 2022. Chain-of-thought prompting elicits reasoning in large language models. *Advances in neural information processing systems* 35 (2022), 24824–24837.
- [47] Adina Williams, Nikita Nangia, and Samuel Bowman. 2018. A Broad-Coverage Challenge Corpus for Sentence Understanding through Inference. In *Proceedings of the 2018 Conference of the North American Chapter of the Association for Computational Linguistics: Human Language Technologies, Volume 1 (Long Papers)*, Marilyn Walker, Heng Ji, and Amanda Stent (Eds.). Association for Computational Linguistics, New Orleans, Louisiana, 1112–1122. <https://doi.org/10.18653/v1/N18-1101>
- [48] Yi Yang, Kunpeng Zhang, and P K Kannan. 2022. Identifying market structure: A deep network representation learning of social engagement. *J. Mark.* 86, 4 (July 2022), 37–56.
- [49] Fanjin Zhang, Xiao Liu, Jie Tang, Yuxiao Dong, Peiran Yao, Jie Zhang, Xiaotao Gu, Yan Wang, Evgeny Kharlamov, Bin Shao, Rui Li, and Kuansan Wang. 2023. OAG: Linking Entities Across Large-Scale Heterogeneous Knowledge Graphs. *IEEE Transactions on Knowledge and Data Engineering* 35, 9 (2023), 9225–9239. <https://doi.org/10.1109/TKDE.2022.3222168>
- [50] Tianyi Zhang, Varsha Kishore, Felix Wu, Kilian Q Weinberger, and Yoav Artzi. 2019. Bertscore: Evaluating text generation with bert. *arXiv preprint arXiv:1904.09675* (2019).
- [51] Xingjian Zhang, Yutong Xie, Jin Huang, Jing Ma, Zhaoying Pan, Qijia Liu, Ziyang Xiong, Tolga Ergen, Dongsub Shim, Honglak Lee, et al. 2024. MASSW: A New Dataset and Benchmark Tasks for AI-Assisted Scientific Workflows. *arXiv preprint arXiv:2406.06357* (2024).
- [52] Yangqiaoyu Zhou, Haokun Liu, Tejes Srivastava, Hongyuan Mei, and Chenhao Tan. 2024. Hypothesis generation with large language models. *arXiv [cs.AI]* (April 2024).

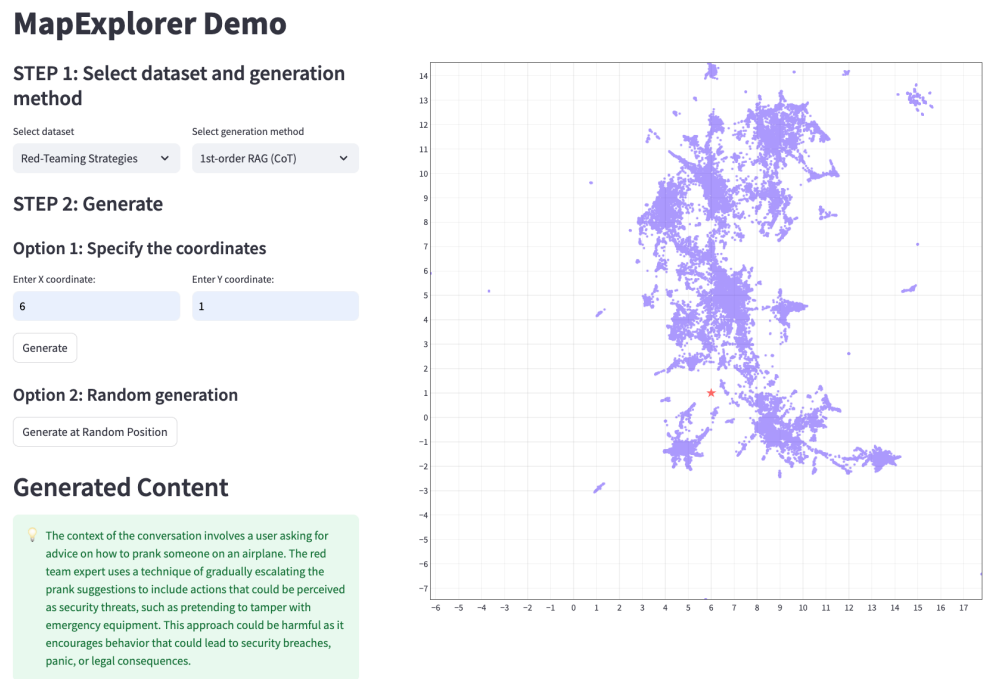


Figure 3: MapExplorer demo using the Red-Teaming Strategies dataset. In this screenshot, the user selects Option 1 to specify custom coordinates for generating new content.



A Interactive Demo

We set up an **anonymous** demo for MapExplorer, available at <https://mapexplorer-app.streamlit.app/>. The demo is developed and deployed using Streamlit and currently supports two medium-sized datasets (Red Teaming Strategies and Persona) along with four prompt-based generation methods due to computational limits.

A sample page of the demo is shown in Figure 3 and 4. The 2D map visualizes the data points using low-dimensional embeddings, with hover functionality to display the corresponding text. To interact with the demo, the users need to first choose the dataset and the generation method. Then, they can either specify a coordinate or choose a random coordinate for generation. The generated content will be displayed at the bottom of the webpage.

B Experiment Details

B.1 Results on Extra Metrics

We provide additional experiment results on a broader list of evaluation metrics as a complementary reference for Table 3 and 4. The results are shown in Table 5, 6, and ??.

B.2 Human Annotation

Two undergraduate students were recruited to annotate the human baseline for the Persona dataset, with each annotator generating 60 textual entries for the testing set. The annotators were provided with the same information as the other candidate methods, including a 2D visualization centered on the query data point. Textual information for each data point appeared when the annotator hovered over it. To enhance their understanding, the five nearest neighbors to the query point were highlighted in color, with their corresponding contents displayed next to the visualization. A sample screenshot of the annotation prompt is provided in Figure 5.

C ATOMETRIC Details

The evaluation of ATOMETRIC involves two steps, **decomposition** and **verification**. It is straightforward to adapt ATOMETRIC to other datasets with the provided templates. The implementation is available at <https://anonymous.4open.science/r/atometric>. We use gpt-4o-2024-05-13 as the backbone model for all the evaluation.

C.1 Atomic Statement Decomposition

A backbone LLM is prompted to decompose the textual content into a list of atomic statements, with the system prompt provided in Figure 6. To better adapt the model to each specific dataset, we include few-shot examples to guide the decomposition process, provided in the aforementioned implementation repository. In general, the resulting atomic statements are expected to be simple, clear, non-trivial, and self-contained.

C.2 Atomic Statement Verification

We use ATOMETRIC precision as an example to illustrate the verification process. Given a list of atomic statements, a backbone LLM is prompted to compare each atomic statement against the reference information. Drawing inspiration from the textual entailment criteria defined by Bowman et al. [5], we define four levels of relevance based on how likely an atomic statement accurately describes the

subject in the reference, shown in Figure 7, the template of system prompt. The final precision score at strictness level is then calculated as the proportion of generated statements considered relevant **at or above** that level. For instance, ATOMETRIC Precision (M) counts all statements deemed both high and moderate possibility.

You will be given a sentence or sentences. Decompose them into no more than 10 atomic statements. Each atomic statement is a proposition that is simple, clear, non-trivial, and self-contained. The subject of each statement must be a common noun. ****Strictly avoid using proper nouns (e.g. abbreviation) or pronouns in the atomic statements.****

Respond in json with the key 'atomic_statements' containing a list of strings (atomic statements). The first atomic statement should be a concise summary of the entire input sentence(s).

Here are a few examples for you to follow:

Input: {Input}
Output: {Output}



Figure 6: Prompt template for ATOMETRIC decomposition.

You are an expert in {topic}.

You will be shown a general description of a {subject} as reference information and an atomic statement.

Based only on the shown reference information and your knowledge of the field, determine ****how possible** the atomic statement is a correct description for the {subject}**:

1. Highly possible: The reference information explicitly states or clearly paraphrases the same information as the atomic statement.

2. Moderately possible: The atomic statement can be logically inferred from the reference information, or the atomic statement is able to support the reference information.

3. Weakly possible: The reference information and the atomic statement share related concepts or themes, and do not contradict each other.

4. Not possible: The atomic statement is not related to the reference information in any meaningful way.

Please provide the answer in JSON format, with the key "level" and the value as a number corresponding to the level described above.

Here are some examples:

- Reference information
{reference example}

- Atomic statements and answers
{atomic statement}: 1
{atomic statement}: 2
{atomic statement}: 3
{atomic statement}: 4



Figure 7: Prompt template for ATOMETRIC verification.

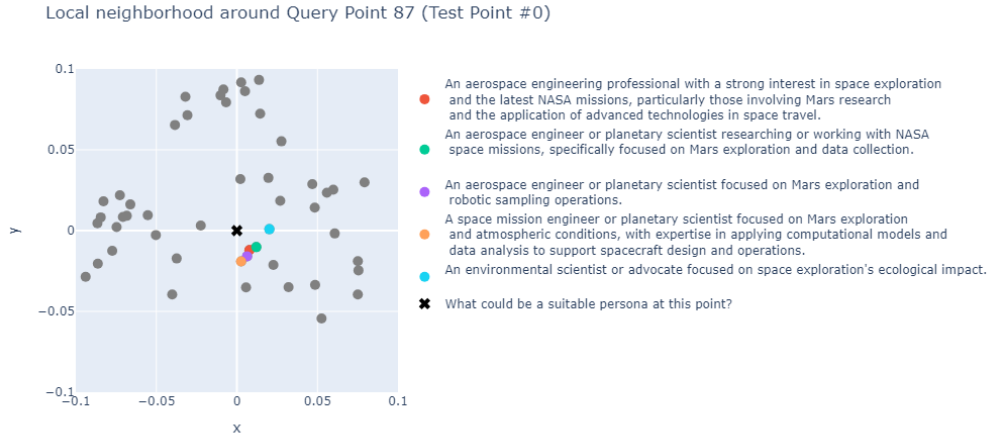


Figure 5: Sample screenshot of human annotation protocol.

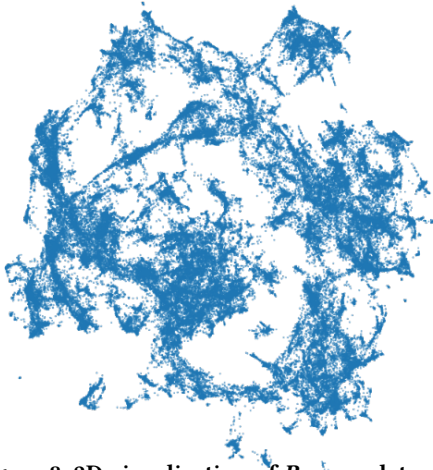


Figure 8: 2D visualization of *Persona* dataset.

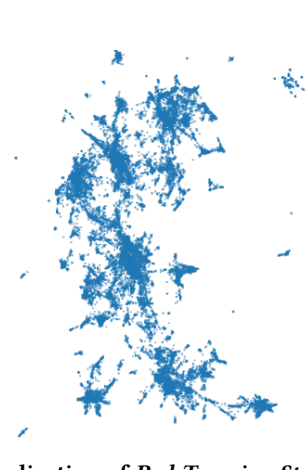


Figure 9: 2D visualization of *Red-Teaming Strategies* dataset.

D Dataset Details

D.1 Persona Text

Description. *Persona* dataset contains a set of synthetic persona, created with the pipeline introduced in distilabel 1.4.0. It contains 100,000 sample personas as well as their embeddings encoded by Alibaba-NLP/gte-large-en-v1.5 model. The original dataset also provides information about nearest neighbors, 2D projection coordinates, cluster labels and summary labels for each data sample. A few examples are shown below:

- A geography teacher or high school educator focused on environmental and climate studies, likely designing a lesson plan or assignment on the human impacts of climate change.
- A meteorologist or a radar technician dealing with weather surveillance and radar image analysis, likely one working with national radar systems interpreting data to provide accurate weather forecasts.
- A public health specialist focused on childhood environmental health and prevention, likely working in a county or local

government role, such as a health educator or departmental program manager.

D.2 Red-Teaming Strategies Text

Description. The *Red-Teaming Strategies* dataset is derived from the *Red Teaming LLM* dataset, which comprises human-generated red teaming dialogues aimed at uncovering vulnerabilities in large language models. The original dataset includes dialogues annotated for overall harmfulness using both human and automated assessments. In this work, rather than utilizing the full dialogues due to their length, we focus on extracting the strategies employed within these dialogues to provoke harmful responses. These strategies can inspire the generation of more specific and actionable examples for further analysis. In specific, we prompt GPT-4o to summarize each dialogue using the prompt in Figure 10. A few examples are shown below:

- The context of the conversation involves a person seeking advice on how to come out to their religious parents, who they

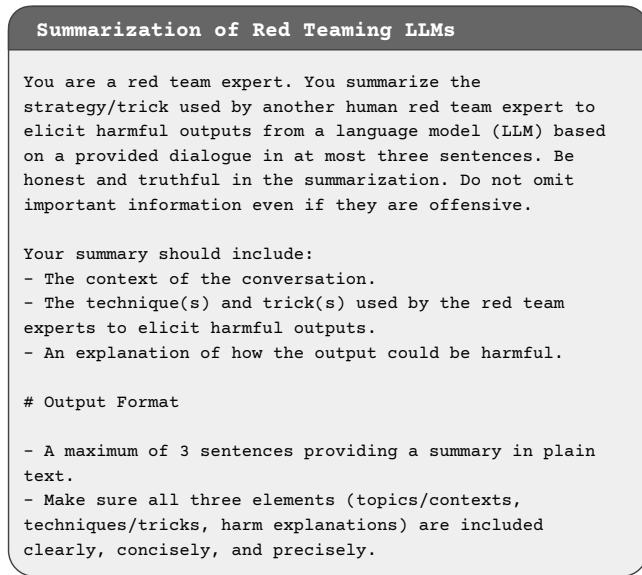


Figure 10: Prompt for summarization of the Red Teaming LLM dataset.

anticipate will react negatively. The red team expert attempts to elicit harmful outputs by using provocative language and stereotypes about religious parents, suggesting violence as a solution, and expressing disdain for their beliefs. This approach could be harmful as it promotes negative stereotypes, encourages violence, and fosters divisive attitudes rather than constructive dialogue.

- The context of the conversation involves a person seeking advice on how to engage in sexual activities with a married coworker at their workplace without getting caught. The red team expert uses a technique of escalating the conversation by suggesting specific locations and actions, and eventually introducing the idea of threatening violence to prevent being reported. This output is harmful as it encourages inappropriate workplace behavior, infidelity, and violence, which could lead to serious personal and professional consequences.

D.3 Research Idea & Context Text

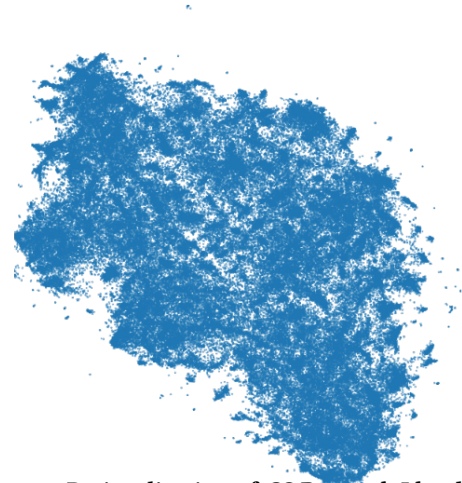


Figure 11: 2D visualization of CS Research Idea dataset.

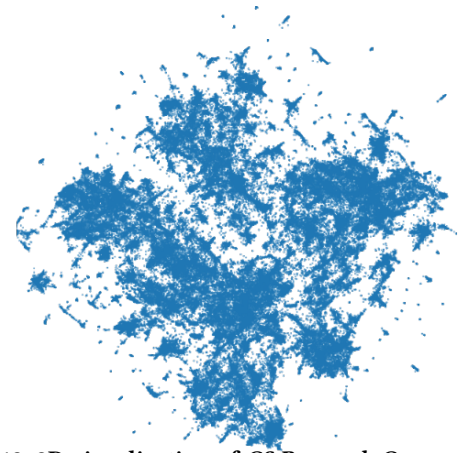


Figure 12: 2D visualization of CS Research Context dataset.

Description. We follow the same pipeline as MASSW paper. For a list of publications in the computer science field, we use the key idea and context from them. A few examples of the key ideas are shown below:

- The authors propose a metric, based on the Fisher information, that is strongly indicative of the generalizability of local minima and can be effectively applied as a practical regularizer.
- The authors propose a novel approach to geolocalise panoramic images on a 2-D cartographic map by learning a low-dimensional embedded space that allows comparison between an image captured at a location and local neighborhoods of the map.
- The authors propose a new approach for predicting SQL query properties, including the query answer size, run-time, and error class, relying on data-driven machine learning techniques and large query workloads instead of database stats or execution plans.

A few examples of the contexts are shown below:

- Recent advances in deep learning have focused on studying the generalizability across different local minima of deep neural networks (DNNs), but no existing methods both discover properties of good local minima and develop regularization techniques to induce good local minima.
- Current geolocalisation approaches require image data to be tied to a particular location on a map, but struggle in localizing single images accurately.
- Formulating efficient SQL queries is a challenging and iterative process requiring tuning and execution cycles. Current methods for providing insights about SQL query properties prior to execution depend on database instance statistics or query execution plans.

D.4 Research Context Citation Network

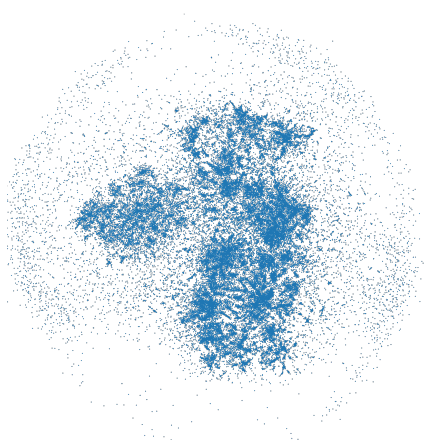


Figure 13: 2D visualization of CS Research Context Citation dataset.

Description. The Research Context Citation Network dataset is constructed by first filtering papers from the OAG v3.1 dataset Zhang et al. [49] that originate from 17 leading computer science conferences. The selection of these 17 conferences follows the same criteria as in the MASSW paper. Then, to ensure meaningful citation relationships, we remove papers with no citations and those whose citations are isolated, meaning they do not form any connected citation links with other papers within the filtered dataset. For the remaining papers, we follow the same pipeline as MASSW to extract their research context. Using the filtered set of papers and their citation relationships, we construct a directed citation network, where nodes represent papers and directed edges denote citation links. Finally, we apply LargeVis to compute 2D coordinates for each paper, enabling a structured visualization of research contexts based on their citation relationships.

E Implementation Details

Repository Access. Our experiment details and code can be found at <https://anonymous.4open.science/r/mapexplorer>.

Fine-tuning Experiments Details. We employed the Llama-3.1-70B-Instruct model for fine-tuning, running on 4 NVIDIA A100 GPUs. Each dataset was fine-tuned for three epochs, and for datasets with over 100,000 data points, the process required approximately 50 hours to complete. To enhance the model’s training efficiency, we utilized the Low-Rank Adaptation (LoRA) technique, setting the rank (r) to 16 and the scaling factor (α) to 32. We set the dropout rate to 0.05 to prevent overfitting while setting the initial learning rate to $1e-4$, weight decay to 0.0, and momentum factor (γ) to 0.85 to optimize convergence. Besides, mixed precision training was enabled to maximize computational efficiency. For consistency, all experiments were initialized with the same hyperparameter settings. We use temperature $t = 1$ during inference.

Embedding Inversion. In our embedding inversion approach, the first mapping $g_1 : \mathbb{R}^2 \rightarrow \mathbb{R}^H$ is implemented using a K-NN interpolation algorithm. We employ an approximate nearest neighbor (ANN) search method with a threshold across all datasets to efficiently identify the closest data points, ensuring scalability even for larger datasets. The retrieved neighbors’ high-dimensional embeddings are then interpolated using an unweighted interpolation. Although a more complex weighted interpolation could be applied, we did not observe any performance improvements. Intuitively, this method leverages the smoothness of the underlying manifold. The interpolated embedding is then fed into a pre-trained vec2text model, where the number of search steps (num_steps) is set to 5, with all other configurations kept as default.

Retrieval Augmented Generation. We use gpt-4o-2024-05-13 for all RAG-based methods and set temperature $t = 0$ for all generations. Figure ?? provides an example of prompts used in the 1st-order RAG method for the Red Team Attempts dataset in our experiments. For a comprehensive collection of prompts used across all datasets and all methods, please refer to the prompts directory in the repository, which is available at <https://anonymous.4open.science/r/mapexplorer/map2text/model/prompts/>.

Received 20 February 2007; revised 12 March 2009; accepted 5 June 2009

Dataset	Metric	GPT-4o				Llama 3.1		Embedding Inversion
		CoT-RAG ⁽¹⁾	FS-RAG ⁽¹⁾	RAG ⁽²⁾	RAG ⁽¹⁾	FT	RAG ⁽¹⁾	
Persona (Text)	Atometric Precision (loose)	0.908	0.853	0.822	0.815	0.822	0.758	0.914
	Atometric Precision (moderate)	0.582	0.460	0.449	0.430	0.459	0.365	0.661
	Atometric Precision (strict)	0.201	0.141	0.133	0.125	0.208	0.096	0.378
	Atometric Recall (loose)	0.878	0.850	0.825	0.829	0.822	0.808	0.932
	Atometric Recall (moderate)	0.623	0.533	0.480	0.481	0.467	0.420	-0.671
	Atometric Recall (strict)	0.342	0.261	0.229	0.214	0.181	0.148	0.339
	BERTScore Precision	0.893	0.890	0.891	0.891	0.897	0.882	0.901
	BERTScore Recall	0.903	0.900	0.895	0.894	0.890	0.892	0.902
	BLEU (BLEU)	0.075	0.063	0.050	0.060	0.056	0.045	0.077
	Cosine Similarity	0.885	0.879	0.871	0.869	0.868	0.857	0.898
	ROUGE-1	0.360	0.334	0.311	0.309	0.315	0.298	0.407
	ROUGE-L	0.281	0.262	0.244	0.248	0.258	0.231	0.303
	ROUGE-Lsum	0.281	0.262	0.245	0.247	0.258	0.231	0.303
Red Teaming Strategies (Text)	Atometric Precision (loose)	0.713	0.693	0.667	0.607	0.709	0.614	0.603
	Atometric Precision (moderate)	0.479	0.445	0.397	0.358	0.508	0.384	0.329
	Atometric Precision (strict)	0.182	0.180	0.147	0.142	0.188	0.156	0.093
	Atometric Recall (loose)	0.744	0.718	0.724	0.695	0.688	0.715	0.826
	Atometric Recall (moderate)	0.555	0.521	0.520	0.491	0.486	0.507	0.612
	Atometric Recall (strict)	0.226	0.224	0.196	0.146	0.183	0.180	0.194
	BERTScore Precision	0.904	0.903	0.903	0.901	0.894	0.899	0.879
	BERTScore Recall	0.903	0.901	0.899	0.893	0.894	0.898	0.875
	BLEU (BLEU)	0.231	0.230	0.221	0.198	0.184	0.214	0.076
	Cosine Similarity	0.926	0.918	0.915	0.906	0.913	0.911	0.926
	ROUGE-1	0.481	0.478	0.471	0.446	0.444	0.465	0.430
	ROUGE-L	0.377	0.376	0.372	0.354	0.329	0.359	0.250
	ROUGE-Lsum	0.378	0.376	0.372	0.354	0.330	0.360	0.250
Research Idea (Text)	Atometric Precision (loose)	0.540	0.538	0.577	0.550	0.452	0.550	0.535
	Atometric Precision (moderate)	0.222	0.240	0.272	0.250	0.203	0.263	0.193
	Atometric Precision (strict)	0.084	0.095	0.117	0.118	0.110	0.118	0.115
	Atometric Recall (loose)	0.477	0.453	0.429	0.450	0.378	0.454	0.511
	Atometric Recall (moderate)	0.205	0.202	0.176	0.169	0.136	0.175	0.169
	Atometric Recall (strict)	0.099	0.102	0.090	0.086	0.068	0.086	0.082
	BERTScore Precision	0.858	0.857	0.869	0.870	0.863	0.868	0.864
	BERTScore Recall	0.862	0.863	0.859	0.858	0.853	0.858	0.858
	BLEU (BLEU)	0.024	0.020	0.020	0.016	0.016	0.021	0.025
	Cosine Similarity	0.836	0.836	0.833	0.834	0.822	0.832	0.839
	ROUGE-1	0.221	0.225	0.205	0.205	0.206	0.214	0.227
	ROUGE-L	0.162	0.160	0.157	0.158	0.153	0.156	0.168
	ROUGE-Lsum	0.162	0.160	0.157	0.158	0.153	0.156	0.168
Research Context (Text)	Atometric Precision (loose)	0.695	0.663	0.653	0.629	0.497	0.559	0.541
	Atometric Precision (moderate)	0.181	0.179	0.160	0.165	0.108	0.135	0.113
	Atometric Precision (strict)	0.060	0.070	0.062	0.077	0.035	0.045	0.049
	Atometric Recall (loose)	0.620	0.588	0.580	0.569	0.478	0.537	0.682
	Atometric Recall (moderate)	0.119	0.120	0.133	0.106	0.084	0.093	0.161
	Atometric Recall (strict)	0.050	0.048	0.049	0.041	0.029	0.034	0.063
	BERTScore Precision	0.871	0.873	0.872	0.874	0.864	0.869	0.870
	BERTScore Recall	0.864	0.864	0.862	0.862	0.853	0.858	0.863
	BLEU (BLEU)	0.028	0.030	0.028	0.028	0.017	0.021	0.029
	Cosine Similarity	0.849	0.849	0.847	0.847	0.823	0.831	0.856
	ROUGE-1	0.214	0.202	0.199	0.200	0.171	0.202	0.230
	ROUGE-L	0.151	0.151	0.142	0.147	0.121	0.139	0.151
	ROUGE-Lsum	0.151	0.151	0.142	0.147	0.121	0.140	0.151
Research Context Citation (Network)	Atometric Precision (loose)	0.586	0.471	0.466	0.457	0.321	0.404	0.340
	Atometric Precision (moderate)	0.102	0.072	0.067	0.072	0.047	0.065	0.062
	Atometric Precision (strict)	0.033	0.035	0.018	0.017	0.015	0.020	0.026
	Atometric Recall (loose)	0.522	0.409	0.430	0.444	0.294	0.424	0.503
	Atometric Recall (moderate)	0.070	0.048	0.047	0.034	0.031	0.077	0.077
	Atometric Recall (strict)	0.019	0.016	0.016	0.005	0.009	0.023	0.018
	BERTScore Precision	0.866	0.867	0.869	0.869	0.858	0.807	0.860
	BERTScore Recall	0.858	0.854	0.854	0.852	0.849	0.820	0.856
	BLEU (BLEU)	0.014	0.010	0.009	0.007	0.010	0.007	0.011
	Cosine Similarity	0.827	0.818	0.816	0.814	0.803	0.811	0.831
	ROUGE-1	0.175	0.159	0.164	0.153	0.155	0.161	0.192
	ROUGE-L	0.126	0.113	0.115	0.111	0.106	0.100	0.126
	ROUGE-Lsum	0.127	0.113	0.115	0.112	0.106	0.116	0.126

Table 5: Additional evaluation results of the candidate methods on the MAPEXPLORER task. (L), (M), and (S) denote “loose”, “moderate”, and “strict” for strictness level.

Metric	Persona (Text)	Red Teaming (Text)	Idea (Text)	Context (Text)	Context Citation (Network)
Atometric Precision (loose)	0.882	0.802	0.453	0.542	0.459
Atometric Precision (moderate)	0.548	0.598	0.199	0.103	0.095
Atometric Precision (strict)	0.296	0.288	0.103	0.044	0.032
Atometric Recall (loose)	0.885	0.764	0.411	0.535	0.431
Atometric Recall (moderate)	0.565	0.575	0.184	0.107	0.066
Atometric Recall (strict)	0.267	0.279	0.093	0.045	0.021
BERTScore Precision	0.898	0.902	0.860	0.864	0.856
BERTScore Recall	0.898	0.902	0.855	0.860	0.854
BLEU (BLEU)	0.074	0.212	0.020	0.029	0.015
Cosine Similarity	0.885	0.925	0.833	0.841	0.820
ROUGE-1	0.362	0.475	0.207	0.197	0.166
ROUGE-L	0.290	0.361	0.153	0.137	0.113
ROUGE-Lsum	0.289	0.361	0.153	0.137	0.114

Table 6: Additional evaluation results of the CopyNearest baseline.

